iJRASET
International Journal For Research in Applied Science and Engineering Technology

INTERNATIONAL JOURNAL FOR RESEARCH

IN APPLIED SCIENCE & ENGINEERING TECHNOLOGY

Volume: 6 **Issue:** IV **Month of publication:** April 2018

DOI: http://doi.org/10.22214/ijraset.2018.4663

www.ijraset.com

Call: 08813907089 | E-mail ID: ijraset@gmail.com

International Journal for Research in Applied Science & Engineering Technology (IJRASET)
ISSN: 2321-9653; IC Value: 45.98; SJ Impact Factor: 6.887
Volume 6 Issue IV, April 2018- Available at www.ijraset.com

A Case Study in Hardening of Cd-Ag Alloys with Solute Concentration

Punarbasu Bose
Department of Physics, Hooghly Women's College, Hooghly, W.B., India

Abstract: ***Quantitative phase abundance and microstructure parameters of different phases in six CdAg alloy compositions prepared at different phase boundary has been estimated using Rietveld's whole profile refinement method. Compositions are found to have mixed phases. Microhardness values for different compositions are found to increase linearly with solute (Ag) concentration when amount of solute is much less compared to solvent. Defect microstructure and microhardness values of these multiphase alloys increase basically due to presence of different types of secondary phases. With increase in solute concentration beyond 17.4% increase in microhardness is less than that expected. Again when solute concentration is nearly 50% the microhardness increase immensely. Such variation of microhardness is explained in the light of co-growth of bcc and hcp phases along the common closest packed planes between the two phases*** $(101)_\beta \parallel (0001)_\alpha$.

Keywords: CdAg Alloys, mixed phase, defect microstructure, microhardness, bcc-hcp co-growth.

I. INTRODUCTION

The ability of a crystalline material to plastically deform largely depends on the ability for dislocation to move within a material. Therefore, impeding the movement of dislocations will result in the hardening of the material. There are a number of ways to impede dislocation movement, which include:

1) controlling the grain size (reducing continuity of atomic planes)
2) strain hardening (creating and tangling dislocations)
3) alloying (introducing point defects and more grains to pin dislocation) [1]

Micromechanical deformation in HCP alloys involves a combination of effects that control component properties. The role of local interfaces and the precise chemistry of different phases in multi-component HCP alloys is an exciting prospect for further study. Hexagonal symmetry leads to considerable anisotropy in the elastic and plastic mechanical properties of HCP metals, as well as other physical properties. The slip systems have been identified as playing a significant role in the plastic deformation of HCP metals and alloys. Microhardness means resistance to dislocation motion. Often Vicker's Micro-hardness values are used as a measure for micromechanical deformation of an alloy. In the present study, six compositions of Cd rich Cd-Ag alloys near to different phase boundary, along with the pure Cd (both in annealed and in cold-worked states) are studied primarily to investigate variation of microhardness in different compositions with increasing solute (Ag) concentration

II. EXPERIMENTAL DETAILS

Following six different compositions of Cd-Ag alloys (TABLE I) in the Cd-solid solution range (η,ε,β'-phases as mentioned in phase diagram (Fig. 1)) and in the mixed phase region (on phase boundary) were prepared from spectroscopically pure metals supplied by M/s Johnson, Matthey and Co., Ltd., London.

TABLE II SOLID SOLUTION COMPOSITIONS

Compositions (wt%)	Melting temp. (K)	Homogenization temp. (K)	Phases	Remarks
Cd- 1.95Ag	673	523	η	hcp1; c/a=1.86
Cd- 3.85Ag	673	523	η+ε	hcp1; c/a=1.87 (hcp2) c/a=1.56
Cd-17.4Ag	873	648	ε	hcp2; c/a=1.56
Cd-29.4Ag	873	648	ε+γ	hcp2; c/a=1.57 γ (ordered bcc Ag_5Cd_8)
Cd-44.85Ag	873	648	$\beta'+\beta_1$	β′ (bcc AgCd) β_1 (hcp2; c/a=1.59)
Cd-48.7Ag	873	648	ε+γ+β′	β′ (bcc AgCd), γ (ordered bcc Ag_5Cd_8), ε hcp2;

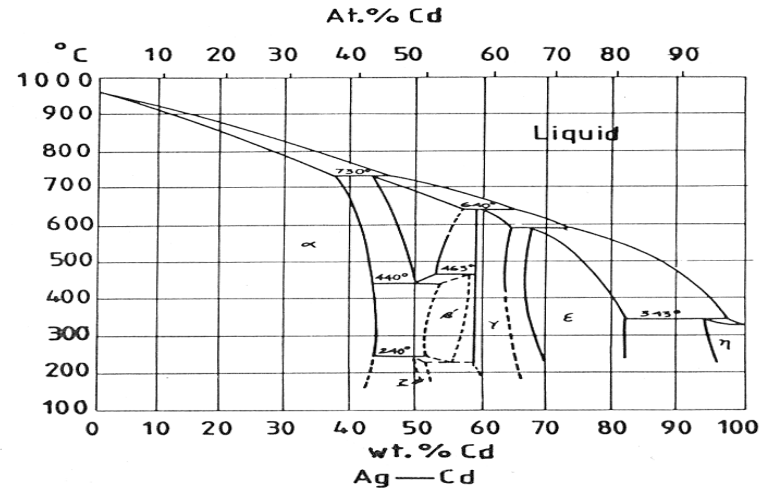

Fig.1 AgCd phase diagram

The x-ray powder diffraction data of both the cold-worked and annealed powder samples and specially processed Si-powder [2] sample (instrumental standard) were recorded in step-scan mode (step size 0.02^0 2θ and counting time 15-20s depending on the peak intensity) using Ni-filtered CuK$_\alpha$ radiation from a highly stabilized Philips x-ray generator (PW 1130) operated at 40kV and 25 mA, coupled with a Philips x-ray powder diffractometer (PW 1710), following the procedure as adopted earlier [3-7].

Accurately weighed quantities of the constituent materials of required compositions (wt%) are melted together in quartz capsules sealed under vacuum in the temperature range of 673-873K. The alloy ingots were homogenized at about 2/3 of the melting temperature of the respective alloys, in the temperature range of 523-648K for 10 to 15 days. No significant weight loss was detected except some grain recrystallization for prolonged heating. Cold-working by hand filing, obtaining annealed standard (523-648K for 10h) and preparation of flat diffractometer samples were made following the same procedures as mentioned earlier [8,9].

Vickers Microhardness measurement has been made on the polished parallel faces of as-cast alloy section of ~ 2mm thickness. For optical microscopy and microhardness studies slices of about 2 mm thick section were cut from the ingots with a Buehler Isomet low speed Diamond Saw (Model No : MA 11-1108) runs through a coolant lubricant for dissipation of heat during cutting. Much care was taken to make the faces of the slices perfectly parallel. In order to get perfectly smooth parallel faces the slices were initially polished by fine grain emery papers mounted on a law speed grinding wheel and finally optically polished on a polishing cloth using diamond paste (of 3μ, 1μ, 1/4μ grain diameter) and a lubricating fluid (Hifin Fluid-"OS") mounted on a low speed grinding wheel. Sometimes, chemical polishing was made for some alloys to get perfectly smooth parallel surfaces.

Using Vickers microhardness tester (Carl-Ziess; Model: Jenavert 2000X), the Vickers microhardness H_V was calculated as

$$H_V = 1.8544\ P/d^2 \qquad (1)$$

Where, P is the load applied in Kg and d is the arithmetic average of the two diagonals of the square indentation (Fig 2). The diagonal lengths of the indented impressions have been accurately measured using calibrated micrometer attached to the eyepiece of the microscope. Up to 160 gm of load for an indentation period of 30 seconds have been used for a fixed load. At least ten indentations at different locations of the specimen surface have been averaged for each data to account for local hardness variation. Sometimes, an etched surface was also exposed for microindentations at grains of different phases and also at grain boundaries

Fig.2 Indentation mark on alloy pallet for determination of H_V

High resolution polarised optical microscope with DIK attachment (Carl Zeiss Model: Jenavert 2000X), were used to observe microstructural features of some of the samples.

III. X-RAYS PROFILE ANALYSIS

Characterization of microstructure of the materials has been made employing Rietveld's whole profile fitting method [10, 11] using the software LS1 as developed by Lutterotti *et al.* [11] following the method for studying the microstructure of materials containing preferred orientation.

Using the values of particle sizes and r.m.s. strains from Rietveld analysis the dislocation density (ρ) values have been evaluated. [12, 13]

IV. RESULTS AND DISCUSSIONS

The microstructural evolution resulting from annealed and cold-worked states of six binary compositions of Cd-Ag alloy prepared on or near a number of different phase boundaries, have been investigated by the well-established technique of x-ray diffraction line profile analysis [10, 11, 14, and 15].

The dependence of mechanical properties, microstructural parameters and c/a ratio of hcp phases on solute concentration and phase boundary effect on those parameters has been investigated.

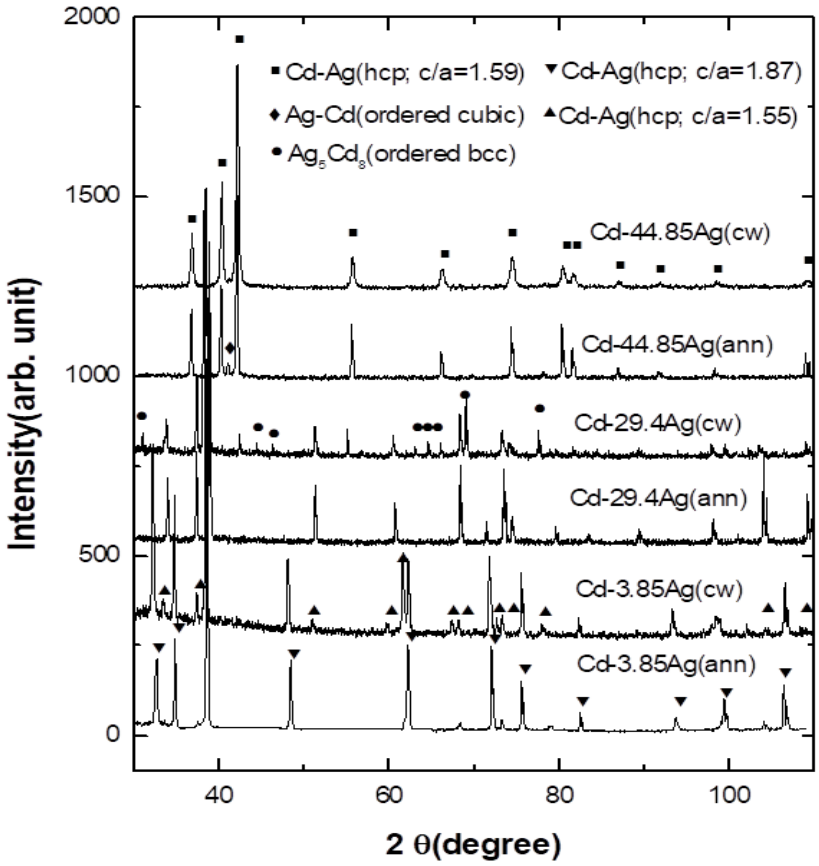

Fig.3 X-ray powder diffraction patterns of Cd-3.85Ag, Cd-29.4Ag Cd-44.85Ag alloys in annealed (ann) and cold worked (cw) state.

The 'a' and 'c' values of the hcp phase (hcp 2) appeared in Cd- 3.85Ag composition and subsequent compositions with higher solute concentration are quite different from the primary solid solution phase hcp 1 and the appearance of this phase may be attributed to sudden expansion of 'a' and contraction of 'c' values of hcp1 phase with increasing solute (Ag) concentration (TABLE III).

Particle size (D_{av}) and r.m.s. strain ($<\varepsilon_L^2>^{1/2}$) values obtained both from Rietveld's analysis [11] are found to be isotropic in nature.

It is also found that particle size of all the phases decrease and r.m.s. strain value increase in cold worked state compared to those of the annealed state which is in agreement with Hall Petch relation [16, 17].

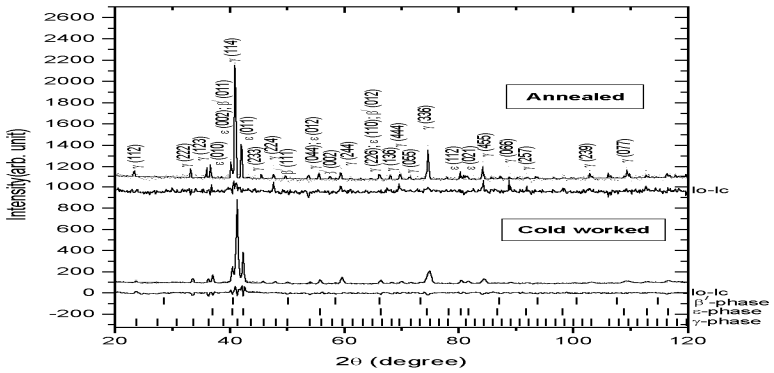

Fig. 4 X-ray powder diffraction pattern of annealed and cold-worked Cd-48.7wt% Ag alloy refined by Rietveld's whole profile fitting analysis.

Experimentally observed values for lattice parameters, isotropic particle size (D_{av}), r.m.s strain $<\varepsilon^2>^{1\backslash2}$ of different phases present in the six Cd-Ag compositions in annealed as well as in coldworked state and Dislocation density (ρ) and Microhardness (Hv) values for respective Cd-Ag compositions has been tabulated in TABLE II

. TABLE II

LATTICE PARAMETERS, MICROSTRUCTURAL PARAMETERS, MACROHARDNESS VALUES FOR DIFFERENT PHASES IN ANNEALED AND COLD WORKED STATE

Composition (wt%)	State of the material	Phase	Lattice parameter (A^0)		c/a	Isotropic particle size D_{av} (A^O)	R.m.s strain $<\varepsilon^2>^{1\backslash2}$ x 10^3	Wt.%	Dislocation density (ρ) x 10^{-11} (cm/cm^3)	Micro hardness (Hv) (kg/mm^2)
			a	c						
Pure Cd	ann	hcp1	2.9771	5.6132	1.886	479.8	0.90	100	0.27	12
	cw	hcp1	2.9821	5.6135	1.882	304.5	1.48	100		
Cd-1.95Ag	ann	hcp1	2.9811	5.5545	1.863	525.5	0.47	100	0.25	19
	cw	hcp1	2.9837	5.5634	1.865	315.6	1.07	100		
Cd-3.85Ag	ann	hcp1 hcp2	2.9773 3.0777	5.5561 4.8129	1.866 1.564	714.7 2500.0	1.01 0.81	91.9 8.1	0.11	26
	cw	hcp1 hcp2	2.9806 3.0918	5.5561 4.8129	1.864 1.557	653.7 1987.7	0.99 0.85	86.4 13.6		
Cd-17.40Ag	ann	hcp2	2.8151	4.3872	1.559	1103.3	0.50	100	0.24	75
	cw	hcp2	2.8211	4.3937	1.557	600.0	0.56	100		
Cd-29.40Ag	ann	hcp2	3.0492	4.8145	1.579	1064.3	0.48	100	0.05	58
	cw	hcp2 cubic	3.0606 9.9956	4.8134	1.574	775.1 1156.5	0.65 0.16	49.6 50.4		
Cd-44.80Ag	ann	hcp2 cubic	2.824 3.1083	4.4809	1.588	580.1 502.4	0.34 2.52	95.7 4.3	1.44	132
	cw	hcp2	2.8255	4.4835	1.587	361.4	2.31	100		
Cd-48.7Ag	ann	bcc (AgCd) ordered bcc (Ag_5Cd_8) ε hcp2;	0.3126 0.9348 0.2828	0.4483	1.5852	298.976 264.853 218.538	0.669 0.07 0.066	15.59 65.34 19.06	2.70	364
	cw	bcc (AgCd) ordered bcc (Ag_5Cd_8) ε hcp2;	0.3173 0.9349 0.2829	0.4501	1.5910	53.998 35.093 44.985	2.731 2.904 1.748	4.36 69.98 25.13		

Phase content and x-ray density of different phases have been estimated from Rietveld analysis and are shown in TABLE IVI. It is interesting to note that as the solute concentration is increased hcp2 phase appeared in the Cd-3.85Ag composition along with major hcp1 phase both in the annealed and cold-worked samples, but with increasing Ag content the hcp1 phase is completely disappears in composition (Cd-17.4Ag). And the phase content of hcp2 phase increases with increasing Ag concentration. At the (ε+γ)-phase boundary (Cd-29.4Ag) the c/a ratio of hcp2 phase has increased to some extent (from 1.56-1.58) and Ag_5Cd_8 (γ-phase, cubic; Z=52) phase appeared only in cold-worked sample. The stored energy gained from the process of cold-working may lead to formation of γ-phase at the expense of modified hcp2 phase. As the stability of γ-phase region (~70-58wt% Ag) is not completely established (isolated by dotted line; in CdAg phase diagram, fig. 1), it appears that the region is composed of modified hcp2 phase and Ag_5Cd_8 phases. Similarly, the $\beta^{/}$ phase region is isolated by dotted lines (fig. 1) and the annealed pattern of Cd-44.85wt% Ag alloy contains reflections of both the modified hcp2 and $\beta^{/}$ phase (cubic, CsCl type) (fig. 3). The phase content of $\beta^{/}$ phase is very small in comparison to modified hcp2 phase, due to cold-working. Unlike the appearance of full-grown $\beta^{/}$ phase by absorbing stored energy, reflections of this phase have been broadened enough beyond detection in cold-worked pattern of the alloy. X-ray density of hcp2 phase is higher than the hcp1 phase, which suggests that the atoms of hcp2 phase are more densely packed than those of the hcp1 phase (TABLE VI).

From the variations of average particle size (D_{av}) and r.m.s. strain values ($<\varepsilon_L^2>^{1/2}$) (TABLE VII) it seems that there is no apparent dependence of variation of these parameters on solute concentration. Defect parameters such as dislocation density (ρ) have been calculated and shown in TABLE VIII. Here, also we found that there is no systematic variation of these parameters on solute concentration.

The maximum (saturated) values of H_v for the alloys varying between 19 to 364 kg/mm^2 (TABLE VIIII) are much higher than the present measured (~12kg/mm^2) and reported values of hardness for pure Cd.

In fig. 5 variation of Microhardness (Hv) values for different Cd-Ag compositions has been plotted with variation of solute concentration (Ag Wt%)

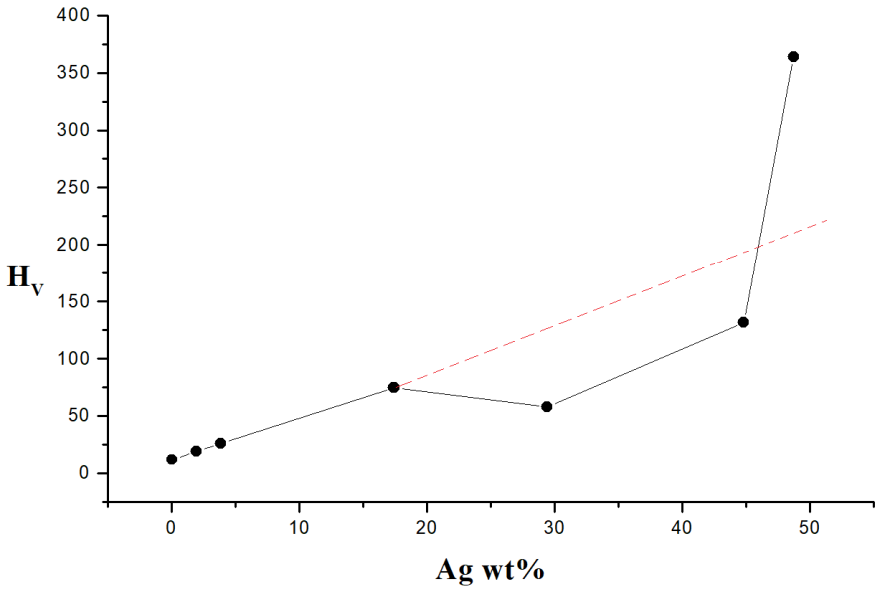

Fig. 5 Variation of saturation microhardness values (H_v) with increasing solute concentration (Ag%)

Looking at variation of saturation microhardness value (H_v) with increasing solute concentration it is found that starting from pure Cd microhardness value (H_v) values for first three compositions (Cd-1.95Ag, Cd-3.85Ag and Cd-17.40Ag) increases linearly with increasing solute concentration. This trend is according to general expectation. The microhardness values (H_v), in general, increase with increasing solute (Ag) concentration, which depicts both the influence of solute concentration and presence of secondary phase in small amount in almost all multiphase compositions. When we extrapolate this trend of variation (shown by dotted line beyond Cd-17.40Ag) departure from this trend is evident in following three compositions. In composition Cd-29.40Ag and Cd-44.80Ag it is

less than that expected from initial trend and in Cd-48.7Ag it is much greater. This is an important observation. Microhardness means resistance to dislocation motions and hence correlates mechanical properties to microstructure in the plastically deformed state of the materials and may be interpreted from the view point of increased generation and mutual interaction among dislocations and other defects, a situation prevalent in polycrystalline materials with increasing indenter load. However, above a critical value of load the dislocation density is reduced due to the onset of dynamic recovery process or cross slip. The present microhardness load characteristics may also be related to the stress field associated with the complex slip process involving two or more sets of intersecting planes (prismatic and pyramidal besides basal) as prevalent in hexagonal materials having c/a ratio appreciably lower than the ideal value. Hexagonal symmetry leads to considerable anisotropy in the elastic and plastic mechanical properties of hcp metals, as well as other physical properties. The slip systems as shown in fig. 5 have been identified as playing a significant role in the plastic deformation of hcp metals and alloys.

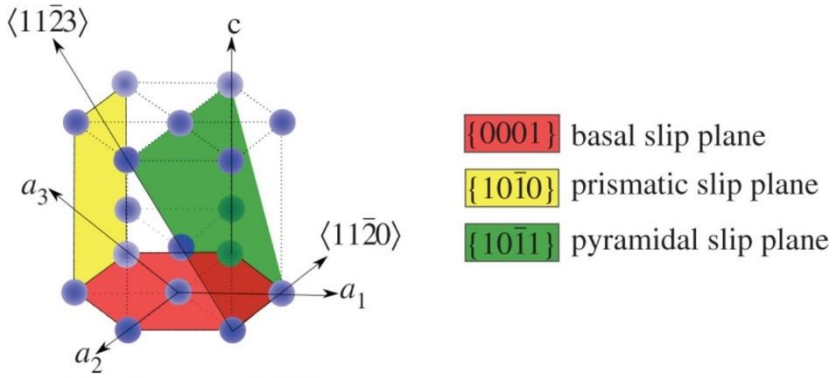

Fig. 5 Major slip planes in hcp lattices

The $\frac{a}{3}\langle 11\bar{2}3\rangle$ or $\langle a\rangle$ directions are the close-packed directions and are thus the shortest Burgers vector possible for perfect dislocations. $\langle a\rangle$ type dislocations have been found to slip on several different slip planes including (0001) basal, $\{10\bar{1}0\}$ prismatic and $\{10\bar{1}1\}$ pyramidal. The three $\langle a\rangle$ Burgers vectors are co-planar within the basal plane and so only offer two independent slip directions. To fully support an arbitrary plastic strain, and so to satisfy the von Mises deformation criterion [18], modes that generate shear displacement out of the basal plane are required. Dislocations with $\frac{a}{3}\langle 11\bar{2}3\rangle$ or $\langle c+a\rangle$ Burgers vectors have been found in many hcp metals and these along with deformation twinning provide the additional deformation modes. The $\langle c+a\rangle$ dislocations have Burgers vectors that are significantly longer than for the $\langle a\rangle$ dislocations and hence are energetically less favoured and tend to have higher resistance to motion. In the present study, for hcp1 phase with c/a ratio > 1.633, slip takes place in the basal plane and for hcp2 phase (Ti, Zr type) with c/a ratio <1.633, slip takes place in the prismatic plane [19].

Another explanation for decrease of microhardness in case of Cd-29.40Ag and Cd-44.80Ag and increase immensely in case of Cd-48.7Ag can be cited from the conclusion of work of Neeraj *et al.*, Suri *et al.* Savage *et al.* and others on the theory of co-growth of bcc and hcp phase [20-26] in Titanium alloy system, where it was assumed a bcc phase and hcp phase can grow simultaneously by sharing common closed packed planes, (111) of bcc (described as β-phase) and (0001) plane of hcp phase (described as α-phase) as schematically drawn in fig. 6.

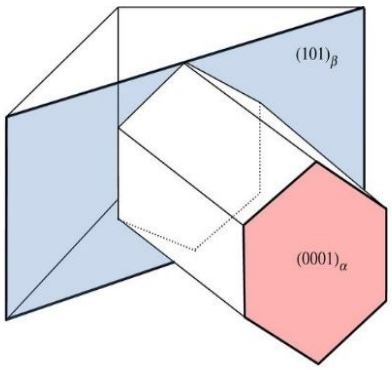

Fig. 6 Co-growth of bcc and hcp phase sharing common closed packed planes, $(111)_\beta$ and $(0001)_\alpha$

They concluded that much of the observed behaviour resulted from the establishment of a Burgers orientation relationship (BOR) between the α-phase hcp orientation and the adjacent transformed β-phase (bcc) orientation, shown schematically in fig. 6. This can be described through the common closest packed planes shared between the two phases $(101)_\beta \parallel (0001)_\alpha$ as well as the sharing of close-packed directions $[111]_\beta \parallel [2110]_\alpha$. The β phase (bcc) has six {101} planes on which up to 12 daughter α variants (hcp) may form. Furthermore, the BOR only has one direct overlap of close-packed directions between the two phases, indicated with an a_1 Burgers vector aligned with b_1. The a_2 direction is closely aligned with the b_2 direction in the parent (111) plane, with typical misalignments of approximately 10° or more. The a_3 direction does not map onto a Burgers vector in the β phase, and the closest vector is a b_3 direction pointing along one [100] direction.

Suri *et al.* [22] argued that slip transmission across the α–β interfaces is strongly dependent on the *a* system orientation with respect to the interface, in the context of the BOR. Furthermore, they did not observe interface sliding. Ankem & Margolin [27] had earlier argued that α–β interface sliding had been observed at room temperature under constant strain-rate loading. Colonies oriented for a_1 slip showed no edge dislocation pile-up and the α–β interface showed little resistance to slip transfer. However, colonies oriented for a_2 showed much edge dislocation pile-up at the α–β interfaces and a correspondingly much higher resistance. Work by Savage *et al.* [25] established that the α–β laths in Ti–6Al–2Sn–4Zr– 2Mo maintain approximately the BOR, and single-colony tests indicated the inhibition of slip transmission for systems in which the α hcp phase was well oriented for basal slip. β-lath shearing was inhibited in these circumstances, but not so for orientations favouring prism slip.

The planar slip observed by Savage *et al.* [24, 25] also occurs near α–β interfaces in single colonies and the stress concentrations which develop at the interfaces were relieved by room temperature creep processes. They showed that in the sample oriented for a_1 basal slip, relatively easy slip transmission occurs across β laths. No pile-ups are observed at interfaces, suggesting stress concentrations are not required to generate slip transmission. However, for basal a_2 and a_3 slip systems adjacent to β laths, higher resistance to slip and stronger strain hardening are observed to occur in single colonies. For a_2 basal slip, no dislocation pile-ups are observed at α–β interfaces. This perhaps the cause of decrease of microhardness and dislocation density in case of Cd-29.40Ag sample as here the phase content of Ag_5Cd_8 (ordered bcc phase) and that of hcp2 phase are same, suggesting co-growth theory of two phases along common closed pack planes. Simultaneous occurrence of two phases is very much evident from the optical micrograph (fig. 7) of Cd-29.40Ag alloy also

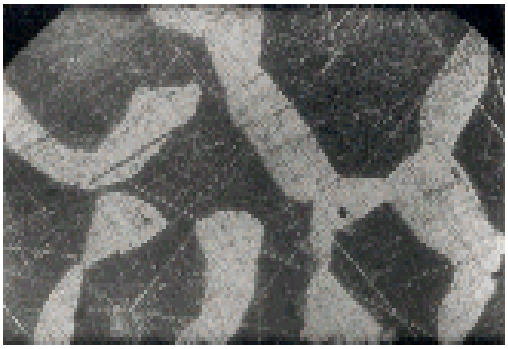

Fig. 7 optical micrograph of Cd-29.40Ag alloy showing co-growth of different phases.

Savage *et al.* [24, 25] also suggested that for thicker β laths dense pile-ups of dislocations are observed at the exit α–β interface, suggesting relatively easy a_2 transmission within the β phase, but difficulty in exiting of b_2 dislocations from the β phase at the α–β interface. For a_3 basal slip, large pile-ups of near-edge a_3 dislocations are observed in the α phase at the α–β interfaces, showing the large resistance to slip developed at the β laths for a_3 basal slip. This is exactly the case in composition Cd-48.7Ag where presence of ordered bcc phase Ag_5Cd_8 is much more (69.98%) than hcp phase (25.13%) suggesting co-growth of hcp phase on thick layers of bcc phase resulting in dislocation pile up at the common bcc hcp interface increasing the value of dislocation density and microhardness abruptly.

V. CONCLUSIONS

Most of the six alloy compositions which are deliberately prepared at different phase boundary regions are found to have mixed phase. Quantitative phase abundance of different phases both in annealed and cold-worked alloys has been estimated using Rietveld's whole profile refinement method. Microhardness values for different compositions are found to increase linearly with solute (Ag) concentration when amount of solute is much less compared to solvent. Defect microstructure and microhardness values

of these multiphase alloys increase basically due to presence of different types of secondary phases. But when solute concentration increases beyond 17.4% increase in microhardness is less than that expected from initial linear trend. Again when solute concentration is nearly 50% the microhardness increase immensely. Such behaviour of change in microhardness value cannot be explained conclusively by the presence of other phase or reduction of particle size or increase in microstrain. Such variation of microhardness may be due to the co-growth of bcc and hcp phases along the common closest packed planes $(101)_{\beta} \parallel (0001)_{\alpha}$ between the two phases as it was observed by several other researchers in titanium rich hcp metal alloys

REFERENCES

[1] William Jr Callister, Materials Science and Engineering, An Introduction. John Wiley & Sons, NY, 1985.
[2] J. G. M. Van Berkum, Ph.D. Thesis, Delft University of Technology, Netherlands, (1994).
[3] H. Pal, S.K. Pradhan and M. De, Materials Transactions, JIM, 36 (1995) 490.
[4] H. Pal, S.K. Pradhan and M. De, Jpn. J. Appl. Phys., 35 (1996) 1836.
[5] S.K. Shee, S.K. Pradhan and M. De, J. Alloys and compounds, 265 (1998) 249.
[6] H. Pal, S.K. Pradhan and M. De, Jpn. J. Appl. Phys., 32 (1993) 1164.
[7] H. Pal, S.K. Pradhan and M. De, Jpn. J. Appl. Phys., 33 (1994) 1443.
[8] S.K. Halder, M. De and S.P. Sen Gupta, J. Appl. Phys., 48 (1977) 3560.
[9] S.K. Ghosh and S.P. Sen Gupta, J. Appl. Phys., 56 (1984) 1213.
[10] H.M. Rietveld, J. Appl. Cryst. 2 (1969) 65.
[11] L. Lutterotti, P. Scardi, J. Appl. Cryst. 23 (1990) 246.
[12] P. Bose, S.K. Shee, S.K. Prahan and M. De, Materials Engineering, 12 (2001) 353
[13] P. Bose, S.K. Shee, S.K. Prahan and M. De, Materials Engineering, 13 (2002) 299
[14] A. Benedetti, G. Fagherazzi, S. Enzo and M. Battagliarin, J. Appl. Cryst., 21 (1988) 543.
[15] R.A. Young and D.B. Wiles, J. Appl. Cryst., 15 (1982) 430
[16] E.O. Hall, Proc Phys Soc London B, 64, 1951; 747.
[17] N.J. Petch, J Iron Steel Inst, 25, 1953; 174.
[18] von Mises, R. Mechanik der festen Körper im plastisch deformablen Zustand. Göttin. Nachr. Math. Phys., vol. 1, (1913) 582.
[19] P. Polukhin, S. Gorelik and V. Vorontsov, Physical Principle of Plastic Deformation, Mir Publishers, Moscow, (1983) p.104,.
[20] T. Neeraj, D.H. Hou, G.S. Daehn, M.J. Mills. Acta Mater. 48 (2000) 1225.
[21] T. Neeraj, M.J. Mills Mater. Sci. Eng. A 319, (2001) 415.
[22] S. Suri, G.B. Viswanathan, T. Neeraj, D-H Hou, M.J. Mills. Acta Mater. 47 (1999) 1019.
[23] T. Neeraj, M.F. Savage, J. Tatalovich, L. Kovarik, R.W. Hayes, M.J. Mills. Philos. Mag. 85 (2005) 279.
[24] M.F. Savage, J. Tatalovich, M.J. Mills. Philos. Mag. 84 (2004) 1127.
[25] M.F. Savage, J. Tatalovich, M. Zupan, K.J. Hemker, M.J. Mills. Mater. Sci. Eng. A 319 (2001) 398.
[26] G. Venkatramani, S. Ghosh, M.J. Mills. Acta Mater. 55, (2007) 3971.
[27] S. Ankem, H. Margolin Metall. Mater. Trans. A 14 (1983) 500.

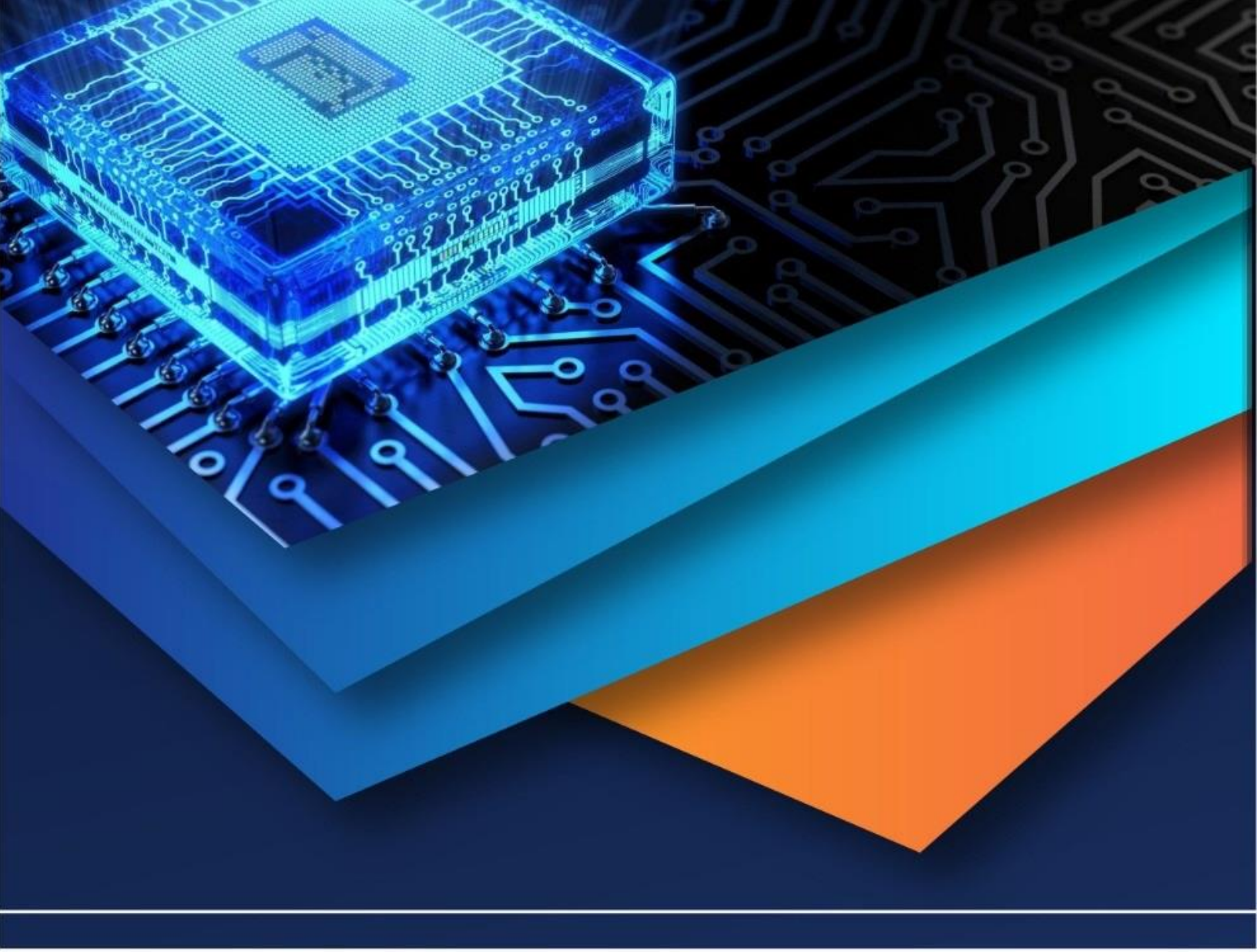

10.22214/IJRASET

45.98

IMPACT FACTOR: 7.129

IMPACT FACTOR: 7.429

INTERNATIONAL JOURNAL FOR RESEARCH

IN APPLIED SCIENCE & ENGINEERING TECHNOLOGY